CSIRO PUBLISHING
www.publish.csiro.au/journals/emu *Emu*, 2010, **110**, 39–47

Adaptation and function of the bills of Darwin's finches: divergence by feeding type and sex

Anthony Herrel[A,B,I], *Joris Soons*[C], *Peter Aerts*[B,D], *Joris Dirckx*[C], *Matthieu Boone*[E], *Patric Jacobs*[F], *Dominique Adriaens*[G] *and Jeffrey Podos*[H]

[A]Département d'Ecologie et de Gestion de la Biodiversité, Museum National d'Histoire Naturelle, 57 rue Cuvier, Case postale 55, F-75231, Paris Cedex 5, France.
[B]Department of Biology, University of Antwerp, Universiteitsplein 1, B-2610 Antwerp, Belgium.
[C]Department of Biomedical Physics, University of Antwerp, Groenenborgerlaan 171, B-2020 Antwerp, Belgium.
[D]Department of Movement and Sports Sciences, Ghent University, Watersportlaan 2, B-9000 Gent, Belgium.
[E]Department of Subatomic and Radiation Physics, Ghent University, Proeftuinstraat 86, B-9000 Gent, Belgium.
[F]Vakgroep Geologie en Bodemkunde, Ghent University, Krijgslaan 281, S8, B-9000 Gent, Belgium.
[G]Evolutionary Morphology of Vertebrates, Ghent University – UGent, K.L. Ledeganckstraat 35, B-9000 Gent, Belgium.
[H]Department of Biology and Graduate Program in Organismic and Evolutionary Biology, University of Massachusetts, Amherst, MA 01003, USA.
[I]Corresponding author. Email: anthony.herrel@mnhn.fr

Abstract. Darwin's finches are a model system for studying adaptive diversification. However, despite the large body of work devoted to this system, rather little is known about the functional consequences of variation in the size and shape of bills. We test, using two methods, if natural or sexual selection, or both, has resulted in functional divergence in bill and head morphology. Firstly, we compare data on head-shape and bite-forces across nine species of Darwin's finches. Secondly, we use micro-CT scans and finite-element models to test the prediction that the shape of the bill in representatives of the different feeding types is adaptively related to use of the bill. Sexual dimorphism in head-shape and bite-force was detected, with females having longer bills than males for a given body size. Moreover, our results show strong differences in bill- and head-morphology between feeding types, with base-crushers having higher bite-forces and also relatively high bite-forces at the tip compared to probers and tip-biters. Finally, our finite-element models suggest that the shape of the bill in the tip-biters and base-crushers confers mechanical advantages by minimising stress in tip-loading and base-loading conditions, respectively, thus reducing probabilities of fracture. Our data support the contention that bill-shape is adaptive and evolves under selection for mechanical optimisation through natural selection on feeding mode.

Additional keywords: bird, bite-force, finite-element modeling, sexual dimorphism.

Introduction

Darwin's finches are a classical model system for the study of adaptive divergence through natural selection (Lack 1947; Bowman 1961) and provide a window on evolutionary processes in action (Grant 1999). Long-term population studies on these animals have been able to show natural selection acting on aspects of morphology, including the size and shape of bills in response to fluctuations in trophic resources (Boag and Grant 1981; Grant and Grant 2002, 2006). Moreover, recent studies have demonstrated how selection on a few key developmental pathways may drive the evolution of bill-shape (Abzhanov *et al*. 2004, 2006). However, despite the large body of work devoted to this system, rather little is known about the consequences of variation in the size and shape of bills on feeding function (but see Bowman 1961), yet understanding the functional role of morphological differences across species and populations is crucial to explain how selection on feeding efficiency (through handling efficiency and seed crushing ability; see Grant 1981) may drive variation in the size and shape of bills in the system (Bowman 1961; Herrel *et al*. 2005*a*, 2005*b*).

Whereas variation in the shape and size of bills across the species of Darwin's finches is mostly continuous (Grant 1999; Foster *et al*. 2008), the bills of Darwin's finches can be subdivided into three functional classes or feeding types: probers, tip-biters and base-crushers (Bowman 1961). The long and pointed bills of probers are predicted to give a functional advantage for probing as, for example, observed in the Common Cactus-Finch (*Geospiza scandens*), which uses its bill to probe cactus flowers (Bowman 1961; Grant 1999). Tip-biters (i.e. the tree-finches (*Camarhynchus* spp.)) have curved upper and lower mandibles, a morphology expected to be specifically suited for applying force at the tip of the bill (Bowman 1961). Base-crushers

 10.1071/MU09034 0158-4197/10/010039

(most ground-finches), on the other hand, have bills that are deep and wide at the base, features that are likely to make the bill well suited to withstand the reaction forces imposed by crushing seeds at the base of the bill. Clearly, both the size and the shape (i.e. including the curvature of the bill in three dimensions) of the bill are important functionally. Yet, despite a careful and detailed analysis of the morphology and function of the bills in Darwin's finches (Bowman 1961), the prediction that the bills of species belonging to different feeding types are functionally adaptive to their ways of feeding remains virtually untested.

Feeding morphology and function might differ not only among species but also by sex. Sexual dimorphism in Darwin's finches has been noted previously for body size (Price 1984*a*) as well as wing-size and wing-shape (Vanhooydonck *et al*. 2009). Sexual dimorphism might emerge through natural selection acting to minimise resource competition between the sexes (Slatkin 1984) or through sexual selection on traits associated with reproductive success (Price 1984*a*; Grant 1999). For example, sexes in the Medium Ground-Finch (*Geospiza fortis*) differ in wing-loading, with males having lower wing-loadings than females, a pattern attributed to the possibility that males benefit from superior manoeuvrability for efficient maintenance of territories (Vanhooydonck *et al*. 2009). If selection on flight-capacity operates differentially between the sexes then, theoretically, differences in head-size and head-shape might be predicted, with males having smaller heads and consequently lower bite-forces and smaller bills than females. This is because having a smaller head would reduce a bird's overall weight and thus improve its stability and manoeuvrability in flight.

Here, we assess patterns of functional divergence in the morphology of bills and heads among nine species of Darwin's finch, and between sexes, and look for signatures of natural or sexual selection, or both, on the cranial system. First, we test for sexual dimorphism in head- and bill-shape, to test whether sexual selection has played a role in the divergence of bill-size and bill-shape. Second, we test whether birds belonging to different feeding types differ in morphology and bite-force as would be expected if bills have adaptively diverged in response to feeding type. Finally, we use mechanical models to test the prediction that bill-shape in representatives of the different feeding types is adaptively related to its use. We use finite-element models, which explicitly take into account the three-dimensional geometry of the bill and allow us to test for mechanical optimisation of biological structures, through comparisons of levels of stress and strain under biologically relevant loading conditions (Richmond *et al*. 2005; Ross 2005).

Materials and methods

Field work was conducted at coastal and upland sites on Santa Cruz Island during February and March of 2003, 2005 and 2006. Individuals of nine Darwin's finch species were captured in mist-nets, banded with unique colour combinations, measured, tested for bite-force, and then released (Table 1). Morphological measurements were taken as described elsewhere (Grant 1999; Herrel *et al*. 2005*a*, 2005*b*) and included bill-length, bill-width, bill-depth, head-length, head-width, head-depth, tarsal length, wing-length (flattened chord), and body mass. Bite-forces were measured using a Kistler force transducer set in a custom-built holder and attached to a handheld Kistler charge amplifier (see Herrel *et al*. 2005*a*, 2005*b*). Birds were induced to bite the force transducer at the back of the jaw where seeds are typically crushed (Herrel *et al*. 2005*a*, 2005*b*) as well as at the front of the jaw. At least three bites at each position were recorded for each individual, of which only the strongest was retained for analysis. Angle of the gape during bite-force measurement was kept consistent across birds by adjusting the distance between the bite plates according to the size of the bird.

Specimens and muscle data

Road-killed specimens were collected during February–March of 2005 and 2006 on Santa Cruz Island, under a salvage permit provided by the Galápagos National Park Service. Intact specimens were collected and preserved in a 10% aqueous formaldehyde solution for 24 h, rinsed and transferred to a 70% aqueous ethanol solution. Specimens were transported to Belgium where one individual of three of the nine Santa Cruz species – Medium Ground-Finch, Common Cactus-Finch (*G. scandens*), and Small Tree-Finch (*Camarhynchus parvulus*) – were scanned at the CT-scanning facility, Ghent University. These three species represent the three main categories of feeding types: base-crusher, prober and tip-biter respectively. A second specimen of each of these three species was dissected and all muscle bundles of the jaw removed individually. Muscles were blotted dry and weighed on a Mettler microbalance (±0.01 mg). Next, muscles were transferred individually to Petri dishes and submerged in a 30% aqueous nitric acid solution for 18 h to dissolve all connective tissue (Loeb and Gans 1986). After removal of nitric acid, muscles were transferred to a 50% aqueous glycerol solution and fibres were teased apart using blunt-tipped glass needles. Thirty fibres were selected from each muscle bundle and drawn using a binocular scope with attached camera lucida. A background grid was also drawn in each image to provide an object for scaling. Drawings were scanned and fibre lengths determined using Scion Image (freely available at http://www.scioncorp.com, accessed January 2010).

Based on muscle mass and fibre length, the physiological cross sectional area of each muscle bundle was determined assuming a muscle density of 1036 kg m^{-3}. Since pennate muscles were separated into their individual bundles, no additional correction for pennation angle was included. Force-generation capacity for each muscle was calculated assuming a muscle stress of 30 N cm^{-2} (Nigg and Herzog 1999). As the external adductor and pseudotemporalis muscles act only indirectly on the upper mandible (Bowman 1961; Nuijens and Zweers 1997; van der Meij and Bout 2004, 2008), the component of the muscle force transferred to the upper mandible was calculated taking into account the position of the muscles and their angles relative to the jugal bone. The pterygoid muscle bundles act directly on the upper mandible (Bowman 1961; Nuijens and Zweers 1997; van der Meij and Bout 2004, 2008), and muscle forces were assumed to be directly transmitted through the pterygoid–palatine complex.

CT scanning and reconstruction

Computerised tomography (CT) scans were conducted at the University of Ghent Computed Tomography (UGCT) scanning

Table 1. Summary of morphometric and bite-force data for the species included in the present study
Means are given ± standard deviation

	Sex (*n*)	Tarsal length (mm)	Bill-length (mm)	Bill-width (mm)	Bill-depth (mm)	Head-length (mm)	Head-width (mm)	Head-depth (mm)	Bite-force at base (N)	Bite-force at tip (N)
Woodpecker Finch (*Cactospiza pallida*)	Male (4)	22.7 ± 0.7	12.3 ± 0.6	7.3 ± 0.1	8.0 ± 0.4	34.6 ± 0.5	15.8 ± 0.6	13.4 ± 2.0	15.0 ± 2.4	10.9 ± 1.9
Small Tree-Finch (*Camarhynchus parvulus*)	Male (17)	20.0 ± 2.0	7.7 ± 0.4	6.4 ± 0.3	7.1 ± 0.3	26.5 ± 0.6	14.0 ± 0.5	12.5 ± 1.4	8.4 ± 1.1	6.1 ± 1.4
	Female (12)	18.9 ± 1.2	7.6 ± 0.4	6.3 ± 0.2	6.8 ± 0.2	26.7 ± 0.9	13.9 ± 0.7	12.4 ± 1.2	8.2 ± 2.6	6.4 ± 2.1
Large Tree-Finch (*Camarhynchus psittacula*)	Male (2)	22.8 ± 1.4	9.4 ± 0.6	7.9 ± 0.7	9.5 ± 0.6	30.6 ± 0.9	15.1 ± 0.7	15.6 ± 1.4	17.8 ± 9.5	12.3 ± 5.9
	Female (1)	20.1	8.2	7.2	7.9	24.4	14.5	12.5	11.8	9.2
Warbler Finch (*Certhidea olivacea*)	Male (16)	19.8 ± 1.0	7.4 ± 0.4	4.4 ± 0.3	3.9 ± 0.2	26.9 ± 1.5	12.4 ± 0.6	10.6 ± 1.1	2.8 ± 0.6	1.6 ± 0.4
	Female (2)	19.6 ± 1.6	7.9 ± 0.4	4.7 ± 0.4	3.9 ± 0.3	28.5 ± 1.1	12.2 ± 0.2	10.0 ± 1.9	3.9 ± 0.1	2.6 ± 0.2
Medium Ground-Finch (*Geospiza fortis*)	Male (213)	21.5 ± 1.7	11.9 ± 1.0	10.0 ± 1.2	11.7 ± 1.3	33.0 ± 2.0	16.0 ± 1.2	15.9 ± 1.3	35.2 ± 14.2	28.3 ± 10.2
	Female (170)	20.8 ± 1.5	12.0 ± 0.9	9.9 ± 1.0	11.5 ± 1.3	32.9 ± 1.6	15.8 ± 1.1	15.7 ± 1.2	32.1 ± 11.9	26.3 ± 9.3
Small Ground-Finch (*Geospiza fuliginosa*)	Male (88)	18.7 ± 1.2	8.5 ± 0.7	6.8 ± 0.4	7.6 ± 1.2	28.0 ± 1.4	13.7 ± 0.8	12.8 ± 1.1	8.3 ± 2.8	7.0 ± 2.4
	Female (27)	18.4 ± 1.3	8.5 ± 0.6	6.6 ± 0.3	7.2 ± 0.4	27.3 ± 2.0	14.6 ± 5.1	12.5 ± 1.1	7.0 ± 2.9	6.1 ± 2.2
Large Ground-Finch (*Geospiza magnirostris*)	Male (15)	24.2 ± 1.5	15.1 ± 0.9	14.0 ± 0.6	16.6 ± 1.2	38.0 ± 1.0	19.7 ± 1.2	19.4 ± 0.7	99.6 ± 24.4	64.8 ± 14.0
	Female (14)	22.7 ± 1.6	14.5 ± 0.8	13.6 ± 0.6	16.0 ± 1.0	37.9 ± 5.8	19.1 ± 1.3	18.9 ± 0.6	91.2 ± 26.3	63.8 ± 15.9
Common Cactus-Finch (*Geospiza scandens*)	Male (47)	21.5 ± 1.4	14.6 ± 0.7	8.2 ± 0.6	9.1 ± 0.5	37.2 ± 1.4	15.0 ± 1.0	14.2 ± 0.9	15.0 ± 5.2	11.7 ± 4.0
	Female (17)	20.6 ± 1.1	14.0 ± 0.5	7.6 ± 0.6	8.3 ± 0.4	36.5 ± 0.8	14.4 ± 1.0	14.8 ± 5.7	11.8 ± 3.6	8.8 ± 2.4
Vegetarian Finch (*Platyspiza crassirostris*)	Male (6)	26.8 ± 1.2	10.7 ± 0.6	9.9 ± 0.3	11.4 ± 0.3	32.5 ± 1.0	17.2 ± 1.2	16.7 ± 1.1	33.6 ± 9.4	27.5 ± 8.8
	Female (12)	26.3 ± 1.7	10.6 ± 0.5	9.7 ± 0.4	11.2 ± 0.7	32.0 ± 0.8	16.7 ± 0.9	16.2 ± 1.0	25.8 ± 7.7	22.2 ± 6.4

facility (www.ugct.ugent.be), using a micro-focus directional type X-ray tube, set at a voltage of 80 kVp and a spot size of 10 µm. Specimens were mounted on a controllable rotating table (UPR160F-AIR, MICOS, Irvine, CA, USA) and fixed in a plastic tube devoid of fluids to increase the contrasts of the reconstructed sections. For each specimen a series of 1000 projections of 940 × 748 pixels was recorded covering 360°. The voxel size ranges from 32 to 55 µm, depending on the specimen (Medium Ground-Finch, 43.73 µm; Common Cactus-Finch, 42.77 µm; Small Tree-Finch, 38.40 µm). Reconstruction of the tomographic projection data was done using the Octopus package (Vlassenbroeck *et al*. 2007), resulting in reconstructed 3D volumes of 940 × 940 × 748 voxels. Volume and surface rendering was performed using Amira 4.1 (64-bit version, Visage Imaging, San Diego, CA, USA).

Finite-element modelling

CT-image sequences were segmented semi-automatically based on grayscale thresholding and smoothed using Amira 4.1 (64-bit version, Visage Imaging), to obtain a triangular surface mesh. Next, a Delaunay tetrahedral volume mesh with a minimum radius-edge ratio of 1.4 was generated in tetgen (Si 2008) and imported in the finite-element program FEBio (Maas and Weiss 2008). Model boundary conditions (Fig. 1*a*) were based on recordings and observations of birds cracking seeds in the field and on dissections. For each modelled specimen, a bite-point was simulated through a translation-constraint of the corresponding elements. Two different bite-points were simulated, a unilateral loading case at the base of the bill on the left side, and a central loading case at the bill-tip. The fronto-nasal hinge was modelled as two rotating but fixed (i.e. no movement allowed) elements. The forces on palatine and jugal bones were applied along the long axis of these bones as determined on the CT-data, and with a magnitude derived from calculated muscle forces. Bone was modelled as a linear elastic, isotropic and homogeneous material with a Young's modulus from 18 GPa, and a Poisson ratio of 0.3 (Yamada 1970; Evans 1973; Vogel 2003).

Linear elements were used in the model, which was solved with an iterative Newton-based Broyden–Fletcher–Goldfarb–Shanno (BFGS) solver. As stress is a complex three-dimensional phenomenon, inherently difficult to interpret, we chose to combine the stresses using the Von Mises criterion. Three areas with high stress were noted in the base-loading condition: posterior on the nasal, and on the ipsi- and contra-lateral processi maxillari of the nasal bone (Fig. 1*b*). An additional high-stress region, the anterior end of the premaxilla, was present when the model was constrained at tip bite-point. Maximal Von Mises stresses were calculated and compared across loading conditions for the different species. Additionally, the external forces needed to satisfy the constraint at the bite-point were derived. The convergence and the stability of the results were tested by an iterative refinement of the mesh up to 700 000 elements and terminated at an accuracy of 10% or better. Finally, finite-element models for Small Tree-Finch and Common Cactus-Finch were scaled by bill-area to the same size as the Medium Ground-Finch model, and simulations were run with input forces based on the Medium Ground-Finch in order to evaluate how bill-shape affects loading of the bill in different loading conditions (tip *v.* base).

Statistical analyses

All morphometric and bite-force data were $\log_{10}$-transformed before analyses. The nine species were then classified into one of three feeding types: tip-biters (Small Tree-Finch and Large Tree-Finch (*C. psittacula*)), base-crushers (Medium Ground-Finch, Small Ground-Finch (*G. fuliginosa*), Large Ground-Finch (*G. magnirostris*) and Vegetarian Finch (*Platyspiza crassirostris*)) and probers (Woodpecker Finch (*Cactospiza pallida*), Warbler Finch (*Certhidea olivacea*), Common Cactus-Finch; see Bowman 1961).

Data were introduced into a multivariate analysis of co-variance (MANCOVA) with sex and feeding type as factors,

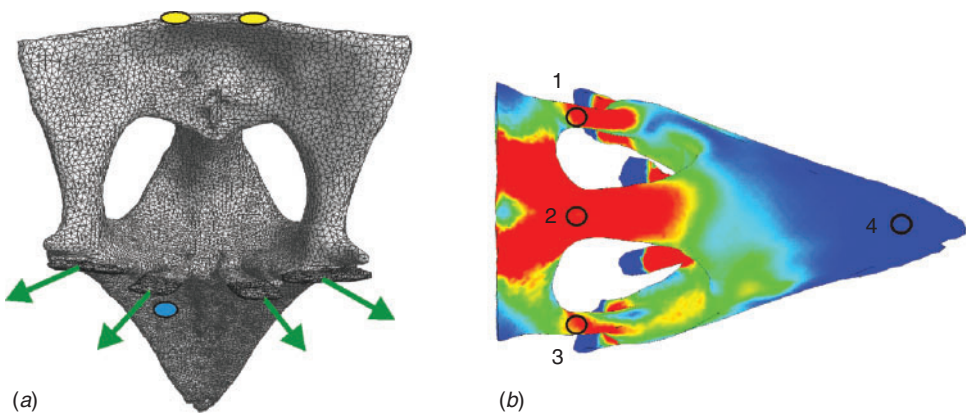

Fig. 1. Schematic representation of the upper mandible (posterior ventral view) (*a*), based on a CT scan, illustrating the boundary conditions of the finite-element model for the Medium Ground-Finch (*Geospiza fortis*). Green arrows represent the muscle forces, the two yellow rotation elements represent the constraints at the fronto-nasal hinge and the blue element represents the bite-point at the base of the bill. Dorsal view of a finite-element model of an upper mandible of the Medium Ground-Finch during a base-loading simulation (*b*). Indicated are the areas of highest stress from which peak stresses are recorded: (1) posterior left; (2) posterior centre; (3) posterior right; (4) anterior centre. A colour version of this figure is available from the journal online.

Table 2. Results of nested ANCOVA with tarsal length as a co-variate and species nested within bite-type testing for differences in morphology and bite-type among feeding types and sexes
Entries in bold denote significant differences

	Species (bite-type)	Sex	Bite-type	Sex × Bite-type
Bill-length	***P*<0.001**	*P*=0.39	***P*<0.001**	*P*=0.85
Bill-width	***P*<0.001**	***P*=0.046**	***P*<0.001**	*P*=0.17
Bill-depth	***P*<0.001**	*P*=0.63	***P*<0.001**	*P*=0.10
Head-length	***P*<0.001**	*P*=0.73	***P*<0.001**	*P*=0.95
Head-width	***P*<0.001**	*P*=0.91	***P*<0.001**	*P*=0.75
Head-depth	***P*<0.001**	*P*=0.43	***P*<0.001**	*P*=0.39
Bite-force at the tip	***P*<0.001**	*P*=0.94	***P*<0.001**	*P*=0.33
Bite-force at the base	***P*<0.001**	*P*=0.61	***P*<0.001**	*P*=0.68
Bite-force at the tip relative to base	***P*<0.001**	*P*=0.33	***P*<0.001**	*P*=0.17

and with tarsal length as co-variate in order to test whether birds belonging to different sexes and feeding types differed in head- and bill-morphology. Next, we ran nested uni-variate analyses of co-variance with sex, feeding type and species nested within feeding type as factors, bill-dimensions, head-dimensions, and bite-force at the tip and at the side as dependent variables, and tarsal length as co-variate. Finally, we tested whether birds of different feeding types were capable of generating relatively larger bite-forces at the tip of the jaw relative to the bite-force they were able to generate at the base of the jaw by running a nested analysis of co-variance (ANCOVA) with feeding type, sex and species nested within feeding type as factors, with bite-force at the tip as the dependent variable, and with bite-force at the side of the jaw and tarsal length as co-variates. Analyses with body mass or wing-length as a co-variate gave similar results in all cases and are not reported here.

Results

Morphometrics and bite-forces

Birds belonging to different feeding types differed in the dimensions of the bill and head (MANCOVA, Wilks' Lambda = 0.18, $F_{12,1302} = 148.3$, $P < 0.001$). Uni-variate nested analyses of co-variance indicated that finches of different feeding types differed in all bill- and head-dimensions (Tables 1, 2). Whereas base-crushers had significantly wider and deeper bills and heads, probers had longer heads and bills. Although the multivariate effect of sex was significant (Wilks' Lambda = 0.98, $F_{6,651} = 2.81$, $P = 0.01$), uni-variate nested ANCOVAs indicated a significant sex effect only for bill-length (Table 2), with females having relatively longer bills than males. The interaction between feeding type and sex was non-significant in all cases.

Birds belonging to different feeding types differed in bite-force, with base-crushers having the highest bite-forces for a given body size (Tables 1, 2). Sexes neither differed in bite-force at the tip, nor in bite-force at the base (Table 2). Bite-force at the tip relative to bite-force generated at the base, and independent of body size, differed significantly between feeding types (Table 2), with base-crushers having the highest bite-force at the tip for both a given side bite and a given body size (Fig. 2).

Finite-element modelling

In all species, stress magnitudes and distributions were found to vary as a function of loading condition. During tip-loading,

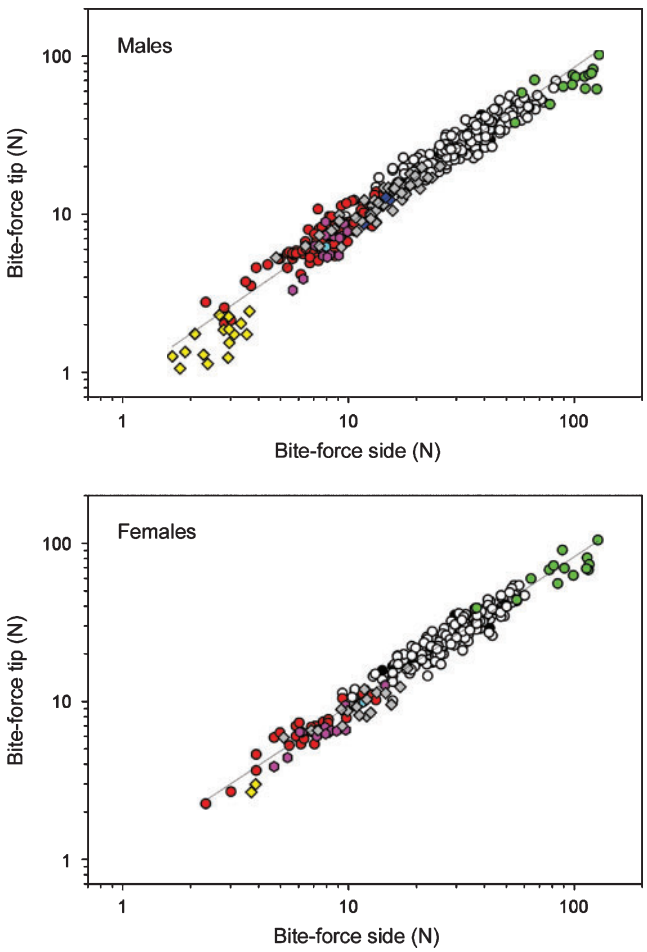

Fig. 2. Scatter plots illustrating the relationship between bite-force at the tip and at the side of the jaw for the different species of Darwin's finch, for males (top) and females (bottom). Symbols represent the different feeding types: circles, base-crushers; diamonds, probers; hexagons, tip-biters. Note how probers have relatively low bite-forces at the tip of their jaws. Species are represented by colours: Warbler Finch (*Certhidea olivacea*), yellow; Woodpecker Finch (*Cactospiza pallida*), blue; Small Tree-Finch (*Camarhynchus parvulus*), pink; Large Tree-Finch (*C. psittacula*), cyan; Medium Ground-Finch (*Geospiza fortis*), white; Small Ground-Finch (*G. fuliginosa*), red; Large Ground-Finch (*G. magnirostris*), green; Common Cactus-Finch (*G. scandens*), grey; Vegetarian Finch (*Platyspiza crassirostris*), black. A colour version of this figure is available from the journal online.

stresses spread across the entire dorsal side of the upper mandible, whereas during base-loading, stresses remain largely confined to the area dorsal and posterior to the external nares (Fig. 3). Additionally, our finite-element models revealed distinct differences in the stress distributions and magnitudes for the representatives of the different feeding types. Both in natural and scaled loading conditions, stresses are notably lower and less widely distributed across the bill for the tip-loading condition in the Small Tree-Finch (a tip-biter) compared to the two other species (Figs 3, 4; Table 3). During base loading, stresses are

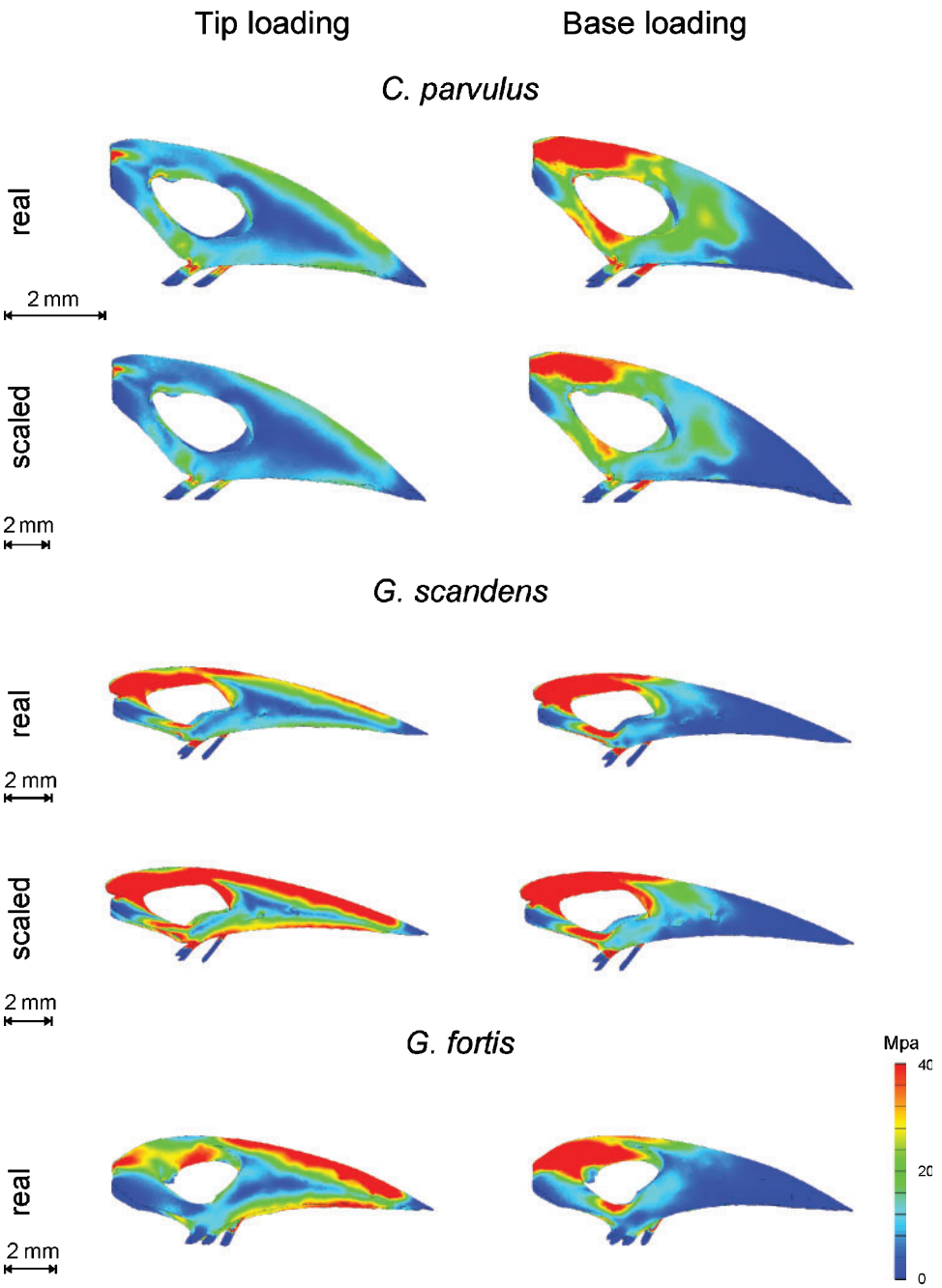

Fig. 3. Lateral view of the upper mandibles of Small Tree-Finch (*Camarhynchus parvulus*), Common Cactus-Finch (*Geospiza scandens*) and Medium Ground-Finch (*G. fortis*) illustrating the output of the finite-element modelling. Warmer colours represent higher stresses. The results of tip-loading conditions are show on the left, base loading on the right. For the Small Tree-Finch and Common Cactus-Finch the results of models using species-specific input data and a scaled version of the model are indicated. The scaled models use input forces based on the Medium Ground-Finch and are scaled to the same surface area. Note how stresses are relatively low under tip-loading conditions in the Small Tree-Finch and relatively low under base-loading conditions in the Medium Ground-Finch. A colour version of this figure is available from the journal online.

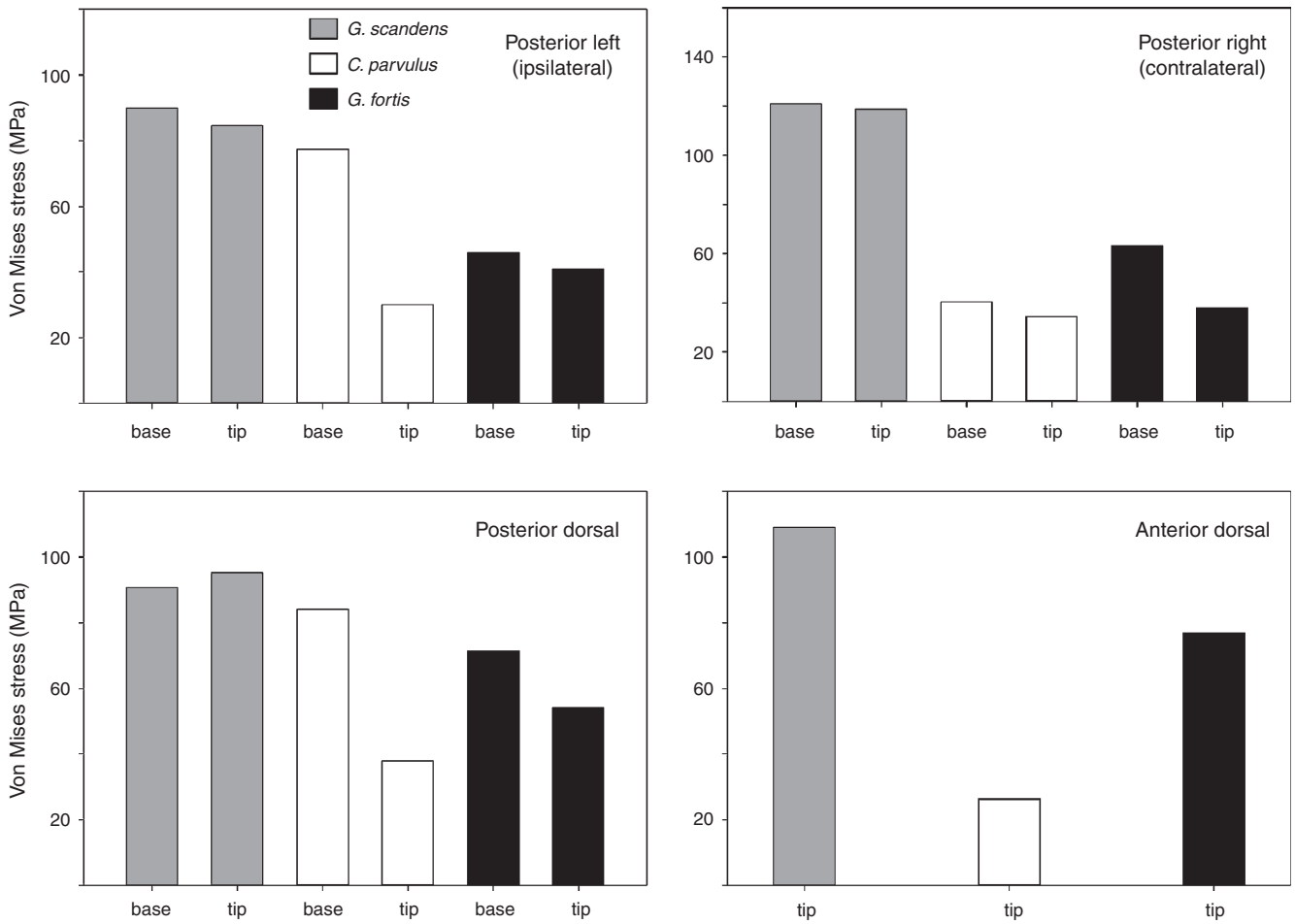

Fig. 4. Graphs illustrating the differences in stress magnitude (Von Mises stress) in the different loading conditions and for different areas of the bill where stresses are highest. All models were scaled to the Medium Ground-Finch (*Geospiza fortis*) model by surface area and use input forces from the latter species as input. Since no high-stress concentrations were observed in the base-loading condition at the anterior dorsal side of the bill no stresses were measured at this location in this loading condition. Note that whereas the model with the shape of the bill of the Small Tree-Finch (*Camarhynchus parvulus*) performs best (low peak stress) under tip-loading conditions, the model with the Medium Ground-Finch shape performs best under base-loading conditions.

generally lowest in the base-crushing Medium Ground-Finch (Table 3) and confined to the posterior aspect of the bill. The design of the bill in the Common Cactus-Finch, a typical prober, appears least suited to dissipate stresses originating from either tip- or base-loading (Figs 3, 4) and shows comparatively high stresses in both unscaled and scaled models. Interestingly, high stress-magnitudes also occurred during base-loading in the Small Tree-Finch (Table 3).

Discussion

Previous studies have shown sexual dimorphism in Darwin's finches, with males being bigger and having generally larger bills than females (Price 1984*a*). Dimorphism in these traits appears to be ancestral to the radiation of Darwin's finches, and may be maintained largely by selection for small body size (and thus rapid breeding) in females, and by sexual selection for large body size in males (Price 1984*b*). Our analyses of bill-dimensions relative to body size show that sexual dimorphism in the shape of the bill and head is largely absent, suggesting that the shape of the bill and head are mainly evolving under natural selection for food types used by both sexes. However, our data do suggest that females have relatively longer bills than do males for a given body size. As females are smaller than males, their relatively longer bills may give them an advantage in feeding on small seeds during periods of drought, by allowing them to pick up and manipulate the small seeds that remain (Price 1984*a*; Grant 1999). However, this remains to be tested in natural populations.

Species that use their bills in different ways varied in the morphology of their heads and bills, as has been described previously (Bowman 1961). Probers have relatively longer heads and bills for a given body size, compared to tip-biters and base-crushers. Base-crushers on the other hand have wider and deeper heads and bills compared to both probers and tip-biters. Moreover, our data indicate differences in bite-force among feeding types. As expected, base-crushers, which typically crush seeds, have the highest bite-forces. Tip-biters and probers show lower bite-forces. Unexpectedly, however,

Table 3. Summary of the finite-element modelling

The mean peak Von Mises stress is calculated across all areas and gives an idea of the magnitude and variation in stress across the entire bill. Scaled models were scaled to the size of the Medium Ground-Finch model by surface area and use input forces based on muscle dissections from the latter species. Data are peak Von Mises stresses (in MPa); s.d., standard deviation

Species	Loading	Scaling	Posterior left	Posterior right	Posterior centre	Anterior centre	Mean	s.d.
Common Cactus-Finch (*Geospiza scandens*)	Base	No	74	98	65		79	17
	Tip	No	50	77	61	58	62	11
	Base	Yes	90	121	91		101	18
	Tip	Yes	85	119	95	109	102	15
Small Tree-Finch (*Camarhynchus parvulus*)	Base	No	97	53	119		90	33
	Tip	No	42	44	44	33	41	5
	Base	Yes	77	41	84		67	23
	Tip	Yes	30	34	38	26	32	5
Medium Ground-Finch (*Geospiza fortis*)	Base	No	46	63	71		60	13
	Tip	No	41	38	54	77	52	18

base-crushers also show the highest bite-forces at the tip relative to the force at the base, thus suggesting a more even distribution of bite-force generating capacity along the length of the bill. This contrast's with Bowman's (1961) suggestion that tip-biters would be particularly proficient in applying bites at the tip of the jaws, as was inferred based on the more pronounced curvature of upper and lower bill in these species.

Although this result might at first suggest that the shape of the bill in tip-biters is poorly suited for its use, our mechanical analyses provide an alternative explanation that ultimately supports Bowman's (1961) argument that morphological variation in bills is adaptive in nature. During tip-loading simulations, we find that the peak stress magnitudes of tip-biters (i.e. Small Tree-Finch) are considerably lower than in species of other feeding types. Moreover, the distribution of areas with high stress in tip-biters is spatially restricted, as compared to the base-crushing shape of the Medium Ground-Finch and the probing bill morphology of the Common Cactus-Finch. Thus, while tip-biters may not actually be able to apply greater forces, we infer that they are better suited to withstand stresses caused by biting with the tip of the bill, thus mitigating the risk of fracturing of the bill.

The bill morphology of base-crushers like the Medium Ground-Finch, on the other hand, seems particularly well suited to resist unilateral loading at the base of the bill, as indicated by the relatively low stresses confined to the reinforced area around the base of the upper mandible (Bowman 1961). The long and slender bill of probers seems generally less well designed to resist the reaction forces imposed by biting at either the tip or the base of the bill. However, during natural maximal loading conditions (muscles 100% active), peak stresses (see Table 3) remain well within the range of the strength of bone (ranging from 106–224 MPa across a wide range of vertebrates; see Yamada 1970; Nigg and Herzog 1999). Similarly, for the Small Tree-Finch stresses are high during base-loading conditions but remain well within safe limits. Thus, our data suggest that the bills of the different species are mechanically optimised for their everyday use, with the different morphologies giving clear performance advantages in specific loading conditions. These data suggest that under natural loading conditions failure of the bill is likely to be associated with the repeated loading needed to crack hard seeds or with the application of forces on irregularly shaped seeds such as those of *Tribulus* (Grant 1981), which may induce unusual orientations of the food reaction forces. In summary, our data support the thesis that bill-shape is adaptive, and that it evolves under mechanical optimisation through natural selection on feeding mode. How the presence of a keratinous rhamphotheca affects the distribution and magnitude of stresses remains to be evaluated in future studies.

Acknowledgements

We thank S. Maas and J. Weis (University of Utah) for allowing us to use the FEBio software package. Field work was coordinated through the Charles Darwin Research Station and the Galápagos National Park Service (GNPS). We are particularly grateful for the generosity of the GNPS in granting a salvage permit. The authors thank Luis De Leon, Ana Gabela, Andrew Hendry, Mike Hendry, Eric Hilton, Sarah Huber, Katleen Huyghe, and Bieke Vanhooydonck for their assistance in the field. This project was supported by NSF grant IBN-0347291 to J. Podos; by an interdisciplinary research grant of the special research fund of the University of Antwerp to P. Aerts, J. Dirckx, J. Soons and A. Herrel; and by an Aspirant fellowship of the Research Foundation – Flanders to J. Podos.

References

Abzhanov, A., Protas, M., Grant, B. R., Grant, P. R., and Tabin, C. J. (2004). Bmp4 and morphological variation of beaks in Darwin's finches. *Science* **305**, 1462–1465. doi:10.1126/science.1098095

Abzhanov, A., Kuo, W. P., Hartmann, C., Grant, B. R., Grant, P. R., and Tabin, C. J. (2006). The calmodulin pathway and evolution of elongated beak morphology in Darwin's finches. *Nature* **442**, 563–567. doi:10.1038/nature04843

Boag, P. T., and Grant, P. R. (1981). Intense natural selection in a population of Darwin's finches (Geospizinae) in the Galapagos. *Science* **214**, 82–85. doi:10.1126/science.214.4516.82

Bowman, R. I. (1961). Morphological differentiation and adaptation in the Galapagos finches. *University of California Publications in Zoology* **58**, 1–302.

Currey, J. D. (2006). 'Bones: Structure and Mechanics.' (Princeton University Press: Princeton, NJ.)

Evans, F. G. (1973). 'Mechanical Properties of Bone.' (Thomas: Springfield, IL.)

Foster, D., Podos, J., and Hendry, A. P. (2008). A geometric morphometric appraisal of beak shape in Darwin's finches. *Journal of Evolutionary Biology* **21**, 263–275.

Grant, P. R. (1981). The feeding of Darwin's Finches on *Tribulus cistoides* (L.) seeds. *Animal Behaviour* **29**, 785–793. doi:10.1016/S0003-3472(81)80012-7

Grant, P. R. (1999). 'The Ecology and Evolution of Darwin's Finches.' (Princeton University Press: Princeton, NJ.)

Grant, P. R., and Grant, B. R. (2002). Unpredictable evolution in a 30-year study of Darwin's finches. *Science* **296**, 707–711. doi:10.1126/science.1070315

Grant, P. R., and Grant, B. R. (2006). Evolution of character displacement in Darwin's finches. *Science* **313**, 224–226. doi:10.1126/science.1128374

Herrel, A., Podos, J., Huber, S. K., and Hendry, A. P. (2005*a*). Evolution of bite force in Darwin's finches: a key role for head width. *Journal of Evolutionary Biology* **18**, 669–675. doi:10.1111/j.1420-9101.2004.00857.x

Herrel, A., Podos, J., Huber, S. K., and Hendry, A. P. (2005*b*). Bite performance and morphology in a population of Darwin's finches: implications for the evolution of beak shape. *Functional Ecology* **19**, 43–48. doi:10.1111/j.0269-8463.2005.00923.x

Lack, D. (1947). 'Darwin's Finches.' (Cambridge University Press: Cambridge, MA.)

Loeb, G. E., and Gans, C. (1986). 'Electromyography for Experimentalists.' (University of Chicago Press: Chicago, IL.)

Maas, S., and Weiss, J. A. (2008). 'FEBio: Finite Elements for Biomechanics. User's Manual, Version 1.0.' Available at http://mrl.sci.utah.edu/uploads/FEBio_um.pdf [Verified 14 January 2010].

Nigg, B. M., and Herzog, W. (1999). 'Biomechanics of the Musculo-skeletal System.' (Wiley: New York.)

Nuijens, F. W., and Zweers, G. A. (1997). Characters discriminating two seed husking mechanisms in finches (Fringillidae : Carduelinae) and estrildids (Passeridae: Estrildinae). *Journal of Morphology* **232**, 1–33. doi:10.1002/(SICI)1097-4687(199704)232:1<1::AID-JMOR1>3.0.CO;2-G

Price, T. D. (1984*a*). The evolution of sexual size dimorphism in a population of Darwin's finches. *American Naturalist* **123**, 500–518. doi:10.1086/284219

Price, T.D. (1984*b*). Sexual selection on body size, plumage and territory variables in a population of Darwin's finches. *Evolution* **38**, 327–341. doi:10.2307/2408491

Richmond, B. G., Wright, B. W., Grosse, I., Dechow, P. C., Ross, C. F., Spencer, M. A., and Strait, D. S. (2005). Finite-element analysis in functional morphology. *Anatomical Record* **283A**, 259–274. doi:10.1002/ar.a.20169

Ross, C. F. (2005). Finite-element modeling in vertebrate biomechanics. *Anatomical Record* **283A**, 253–258. doi:10.1002/ar.a.20177

Si, H. (2008). TetGen: a quality tetrahedral mesh generator and three-dimensional Delaunay triangulator. Available at http://tetgen.berlios.de [Verified 14 January 2010].

Slatkin, M. (1984). Ecological causes of sexual dimorphism. *Evolution* **38**, 622–630. doi:10.2307/2408711

van der Meij, M. A. A., and Bout, R. G. (2004). Scaling of jaw muscle size and maximal bite force in finches. *Journal of Experimental Biology* **207**, 2745–2753. doi:10.1242/jeb.01091

van der Meij, M. A. A., and Bout, R. G. (2008). The relationship between shape of the skull and bite force in finches. *Journal of Experimental Biology* **211**, 1668–1680. doi:10.1242/jeb.015289

Vanhooydonck, B., Herrel, A., Gabela, A., and Podos, J. (2009). Wing shape variation in the medium ground finch (*Geospiza fortis*): an ecomorphological approach. *Biological Journal of the Linnean Society* **98**, 129–138. doi:10.1111/j.1095-8312.2009.01269.x

Vlassenbroeck, J., Dierick, M., Masschaele, B., Cnudde, V., Van Hoorebeke, L., and Jacobs, P. (2007). Software tools for quantification of X-ray microtomography at the UGCT. *Nuclear Instruments & Methods in Physics Research. Section A, Accelerators, Spectrometers, Detectors and Associated Equipment* **580**, 442–445. doi:10.1016/j.nima.2007.05.073

Vogel, S. (2003). 'Comparative Biomechanics: Life's Physical World.' (Princeton University Press: Princeton, NJ.)

Yamada, H. (1970). 'Strength of Biological Materials.' (Williams and Wilkins: Baltimore.)

Manuscript received 4 May 2009, accepted 5 September 2009